SOFT DIFFRACTION (THEORY)

Uri Maor

Raymond and Beverly Sackler Faculty of Exact Science

Tel Aviv University, Tel Aviv, 69978, Israel

INTRODUCTION

- **Hard QCD** deals with the strong interactions of high transverse momenta partons. These are short distance phenomena which are calculated within the framework of **pQCD.**

- **Soft QCD** is traditionally associated with low transverse momenta partons separated by large distances. Consequently, we are unable to utilize perturbative methods. The relevant **npQCD** calculations are, thus, based on phenomenological models, foremost, the **Regge pole model in which the Pomeron ($I\!P$) is the leading term.**

- In the first part of my talk I shall specify the architecture of updated $I\!P$ models and how they **change our perception of the traditional Regge model.** In the second part I shall concentrate on the theoretical output and **recent LHC results relevant to this talk.**

POMERON MODEL ARCHITECTURE

Updated Pomeron model have a few components:

- A bare non screened $I\!P$ exchange amplitudes in a 2 channel Good-Walker system composed of elastic and "low mass" GW diffraction.

- Eikonal rescatterings of the incoming projectiles secure that the scattering amplitudes are bounded by s-channel unitarity black disc bound.

- t-channel unitarity is coupled to multi $I\!P$ t-channel interactions leading to "high mass" diffraction and additional screening of the GW sector.

- The survival probability factor, which has an eikonal and a multi-$I\!P$ components, is responsible for the reduction of the non GW diffraction.

- Current $I\!P$ models are coupled to a price tag of non conventional large output of $\alpha_{I\!P}(0)$ and exceedingly small $\alpha'_{I\!P}$. The traditional Regge features are restored by s an t unitarity screenings.

GOOD-WALKER DECOMPOSITION

Consider a system of two orthonormal states, a hadron Ψ_h and a diffractive state Ψ_D. The GW mechanism stems from the observation that these states do not diagonalize the 2x2 interaction matrix T. Assume that T is diagonalized by Ψ_1 and Ψ_2. We get,

$$\Psi_h = \alpha\,\Psi_1 + \beta\,\Psi_2, \quad \Psi_D = -\beta\,\Psi_1 + \alpha\,\Psi_2, \quad \alpha^2 + \beta^2 = 1.$$

The 4 elastic GW amplitudes are

$$A_{i,k}^{i',k'} = \,<\Psi_i\,\Psi_k|\mathbf{T}|\Psi_{i'}\,\Psi_{k'}> = A_{i,k}\,\delta_{i,i'}\,\delta_{k,k'}.$$

For initial $p(\bar{p}) - p$ we have $A_{1,2} = A_{2,1}$. The (i,k) s-channel unitarity equation is analogous to the single dimension equation,

$$Im\,A_{i,k}\,(s,b) = |A_{i,k}\,(s,b)\,|^2 + G_{i,k}^{in}(s,b).$$

$G_{i,k}^{in}$ is the summed probability for all non GW inelastic processes (including non GW "high mass diffraction") induced by an initial (i,k) state.

As in the single dimension equation, we have

$$A_{i,k}(s,b) = i\left(1 - \exp\left(-\frac{\Omega_{i,k}(s,b)}{2}\right)\right), \quad G_{i,k}^{in}(s,b) = 1 - \exp\left(-\Omega_{i,k}(s,b)\right).$$

The b space opacities, $\Omega_{i,k}(s,b)$, are real, determined by the Born input.

The **elastic, SD and DD** amplitudes are:

$$a_{el}(s,b) = i\{\alpha^4 A_{1,1} + 2\alpha^2\beta^2 A_{1,2} + \beta^4 A_{2,2}\},$$

$$a_{sd}(s,b) = i\alpha\beta\{-\alpha^2 A_{1,1} + (\alpha^2 - \beta^2)A_{1,2} + \beta^2 A_{2,2}\},$$

$$a_{dd} = i\alpha^2\beta^2\{A_{1,1} - 2A_{1,2} + A_{2,2}\}.$$

Updated eikonal models are multi channel in which:

$\Omega_{i,k}(s,b) = \nu_{i,k}(s)\,\Gamma_{i,k}(s,b)$. In Regge type models, $\nu_{i,k}(s) = g_i g_k (\frac{s}{s_0})^{\Delta_{\mathbb{P}}}$. $\Gamma_{i,k}(s,b)$ is parameterized so as to reproduce $\frac{d\sigma}{dt}$ of the elastic and diffractive channels in the forward cone. The eikonal re-scatterings of the incoming projectiles are summed over the GW eigen states.
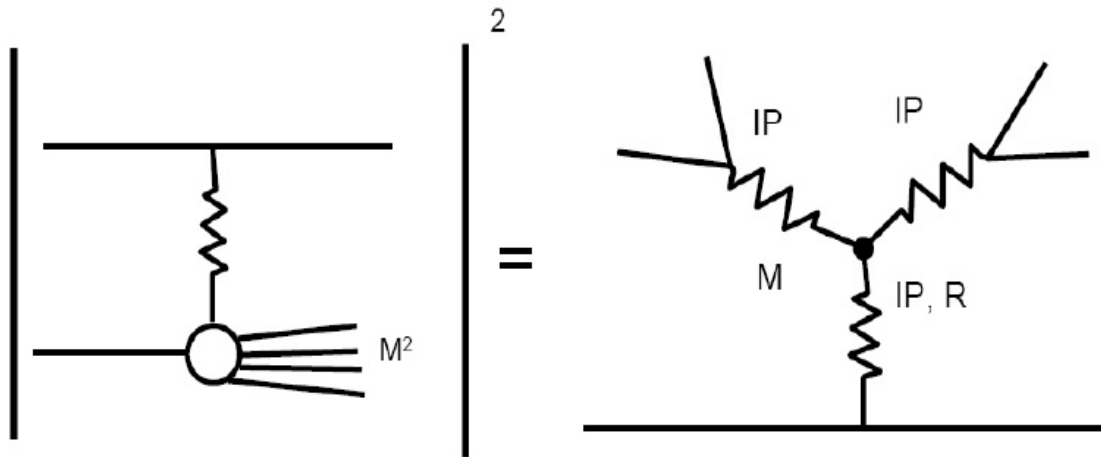
MULTI POMERON INTERACTIONS

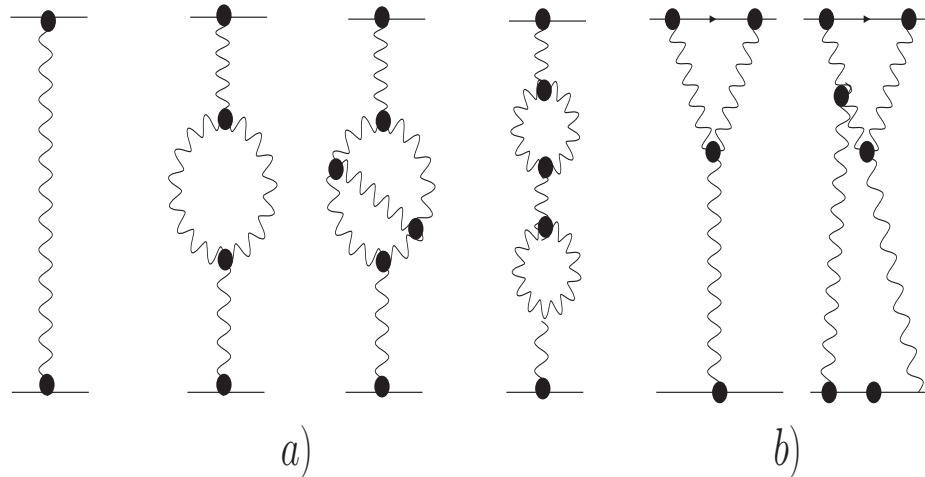Mueller(1971) applied 3 body unitarity to equate the cross section of

$a + b \rightarrow M + b$ to the triple Regge diagram $a + b + \bar{b} \rightarrow a + b + \bar{b}$.

The core of this representation is a triple vertex with a leading $3I\!P$ term.

The equation is valid for "high mass diffraction", $\frac{m_p}{M^2} << 1$ and $\frac{M^2}{s} << 1$.

The corresponding cross section is $M^2 \frac{d\sigma^{3I\!P}}{dt\,dM^2} = \frac{g_p^2(t)g_p(0)G_{3I\!P}}{16\,\pi^2} \left(\frac{s}{M^2}\right)^{2\alpha_{I\!P}(t)-2} \left(\frac{M^2}{s_0}\right)^{\alpha_{I\!P}(0)-1}$.

$\alpha_{I\!P}$ connects σ_{tot} and σ_{el} s dependences and σ_{sd} high mass dependence.

a)   b)

Muller's 3$I\!P$ approximation for **"high mass" single diffraction** is the lowest order of a very large family of multi Pomeron interactions which are not included in the **GW mechanism.** This dynamical feature is compatible with t-channel unitarity. The figure shows the low order **$I\!P$ Green's function.**

a) Enhanced diagrams which renormalize (in low order) the $I\!P$ **propagator.**

b) Semi-enhanced diagrams which renormalize (in low order) the $I\!P$**-p vertexes.**

The complexity of these diagrams requires **summing algorithms** which are **model dependent.**

- The diffractive upper bound is, generally, taken as 0.05s.

- All groups bound the "high mass" diffraction from below by Y = 3, compatible with Mueller's bounds. It corresponds to $M \leq 4.5 GeV$.

- The upper bound on the "low mass" is model dependent. Kaidalov, at the time, bounded the "low mass" diffraction from above by Y = 3. i.e. in his parametrization there is no overlap between the "low" and "high mass." This is practiced also by KMR and Ostapchenko.

- The approach of GLM is radically different. In our model, both GW and non GW diffraction have the same upper bound.

- Consequently, GLM diffraction is predominantly GW while the diffraction of Kaidalov, KMR and Ostapchenko is predominantly non GW.

- In the ISR-Tevatron range the difference between the two definitions is small. At LHC energies the difference becomes significant.
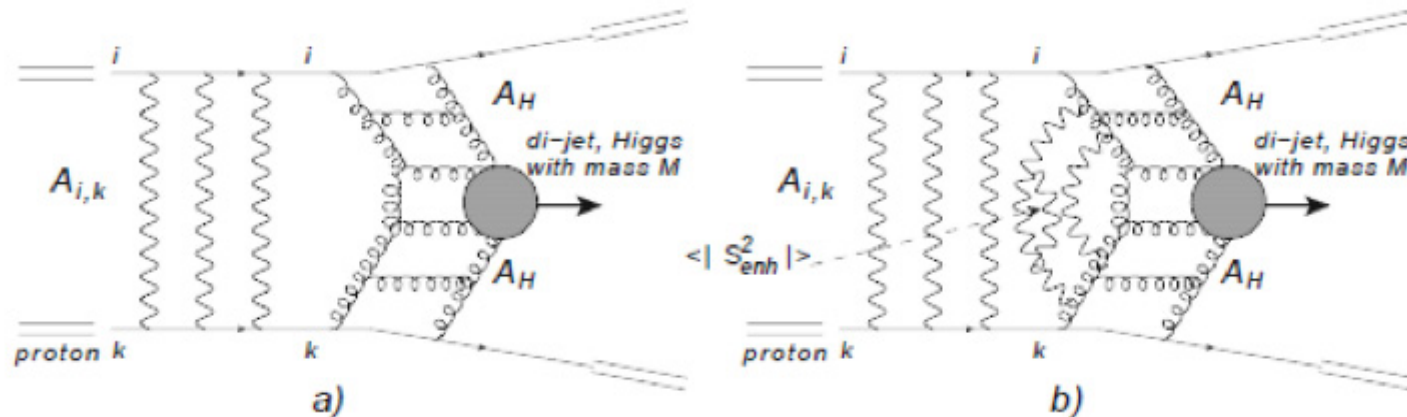
LRG SURVIVAL PROBABILITY

The Pomeron is defined as a moving Regge pole void of electric and color charges. The proposition by Low and Nussinov (1975) that the $I\!\!P$ is a 2 gluon color singlet, is intuitively appealing. This is a Born term description. In high order the 2 gluons are replaced by gluonic ladders.

The coupled experimental signature is a large rapidity gap (LRG) in the $\eta - \phi$ lego plot devoid of hadrons. $\eta = -ln(tan\frac{\theta}{2})$. Screenings of $I\!\!P$ exchange originate from s-channel eikonalization and t-channel multi $I\!\!P$ interactions.

Specifically:

- GW elastic+"low mass" diffraction s-channel unitarity screening is attained through eikonalization.

- Non GW diffraction (including "high mass") is suppressed by the eikonal LRG survival probability factor.

Survival probability for exclusive central diffractive production of the Higgs boson. Fig. a shows the contribution to the survival probability in the G-W mechanism, while Fig. b illustrates the origin of the additional factor $\langle | S^2_{enh} | \rangle$.

- Both GW and non GW cross sections are further screened by multi $I\!P$ t-channel interactions.

- Non GW diffraction (soft or hard) screening is expressed by the survival probability that given LRG's will not be filled by debris (partons and/or hadrons) originating from either the initial projectiles re-scatterings, or the multi $I\!P$ interactions.

The survival probability factor is defined as the ratio between the screened and non screened non GW diffractive cross sections.

Denote the gap survival factor initiated by s-channel soft eikonalization S^2_{eik}, and the one initiated by t-channel multi $I\!\!P$ interactions (soft or hard) S^2_{enh}.

In a frequently used approximation, $S^2 = S^2_{eik} \cdot S^2_{enh}$.

The s and t screenings induce a monotonous decrease of $\triangle^{eff}_{I\!\!P}$ (Pomeron renormalization). Its GLM predictions are shown in the Table.

W[TeV]	$1.8 \rightarrow 14.0$	$14.0 \rightarrow 100.0$
$\triangle^{input}_{I\!\!P} = 0.335$	0.056	0.041
$\triangle^{input}_{I\!\!P} = 0.200$	0.074	0.060

Following I shall discuss mainly **3 multi-channel** $I\!P$ **models in which**
s and t unitarity screenings are incorporated. The models are very similar
conceptually, but differ in their multi $I\!P$ **diagram summation procedures**
and data analyses.

- **GLM(10) (Tel AVIV): has a single soft** $I\!P$**,** $\Delta_{I\!P} = 0.20$**,** $\alpha'_{I\!P} = 0.02$**.**

- **KMR(10) (Durham):** $\Delta_{I\!P} = 0.3$**,** $\alpha'_{I\!P} \propto 1/p_t^2$ **is approximated by 3 effective**
  BFKL like trajectories with different $\alpha'_{I\!P}$ **values.**

- **Ostapchenko(10) (Bergen): has 2 Pomerons,**

  soft: $\Delta_{I\!P} = 0.17$**,** $\alpha'_{I\!P} = 0.11$**,   hard:** $\Delta_{I\!P} = 0.31$**,** $\alpha'_{I\!P} = 0.085$**.**

$\Delta_{I\!P}$ **and** $\alpha'_{I\!P}$ **are just two out of a large number of free parameters determined**
from the adjustment of a small data base. This difficulty was addressed
differently by each group.

PARTONIC STRUCTURE OF THE POMERON

The introduction of multi $I\!P$ interactions as a major component of the Pomeron model, poses a serious problem in as much as it depends on many unknown rapidity space point like couplings corresponding to $nI\!P \to mI\!P$.

The microscopic sub structure of the Pomeron is provided in **Gribov partonic interpretation of Regge theory,** in which the slope of the Pomeron trajectory is related to the mean transverse momentum of the partonic dipoles constructing the Pomeron, and, consequently, the running QCD coupling constant.

$$\alpha'_{I\!P} \propto 1/ <p_t>^2, \quad \alpha_S \propto \pi/ln\left(<p_t^2>/\Lambda_{QCD}^2\right) << 1.$$

- **GLM** utilize the **pQCD MPSI procedure,** where $nI\!P \to mI\!P$ reduces to a sequence of $G_{3I\!P}$ vertexes (Fan diagrams). i.e. $2I\!P \to I\!P$ and $I\!P \to 2I\!P$.

- **KMR** assumed couplings are $g_m^n = \frac{1}{2} g_N \, nm \, \lambda^{n+m-2} = \frac{1}{2} nm \, G_{3I\!P} \, \lambda^{n+m-3}$.
  λ is a free parameter, $n + m > 2$, $G_{3I\!P} = \lambda g_N$. **Kaidalov and Ostapchenko** have the same coupling with a different normalization.

HOW MANY POMERONS?

The 2 significant properties of the Pomeron model, regardless of its version, are a relatively high $\Delta_{I\!\!P}$ and exceedingly small $\alpha'_{I\!\!P}$, which initiate the s and t unitarity screenings. These values are remarkably close to those of the BFKL Pomeron, $\Delta_{BFKL} = 0.2 - 0.35$ and $\alpha'_{BFKL} = 0$.

Recall, though, that The soft $I\!\!P$ is a simple moving pole in the J-plane, while, the BFKL $I\!\!P$ is a branch cut. On the other hand:

- The BFKL $I\!\!P$ is commonly parameterized as a simple J-pole with $\alpha'_{BFKL} = 0$, which is a signature of the hard $I\!\!P$.

- In pQCD the BFKL Pomeron slope
  $\alpha'_{I\!\!P} \propto 1/Q_s^2 \to 0$ as $s \to \infty$. Q_s^2 is the saturation scale.

HERA studies of e-p DIS show a continuous transition from $\Delta_{I\!\!P} \simeq 0.1$ at small Q^2 (large screenings), to $\Delta_{I\!\!P} \simeq 0.4$ at large Q^2 (diminishing screenings).

	1.8 TeV			7 TeV			14 TeV			100 TeV		
	GLM	**KMR**	**OSTAP**	**GLM**	**KMR**	**OSTAP**	**GLM**	**KMR**	**OSTAP**	**GLM**	**KMR**	**OSTAP**
$\sigma_{tot}\,mb$	74.4	72.8	73.0	91.3	89.0		101.0	98.3	114.0	128.0	127.1	
$\sigma_{el}\,mb$	17.5	16.3	16.8	23.0	21.9		26.1	25.1	33.0	35.6	35.2	
$\sigma_{sd}\,mb$	8.9	13.7	9.6	10.2	16.9		10.8	17.6	11.0	12.7	24.7	
$\sigma_{dd}\,mb$	4.5	8.0	3.9	6.4	11.2		6.5		4.8	7.8		
S_H^2	0.11			0.06	0.024		0.04	0.015				
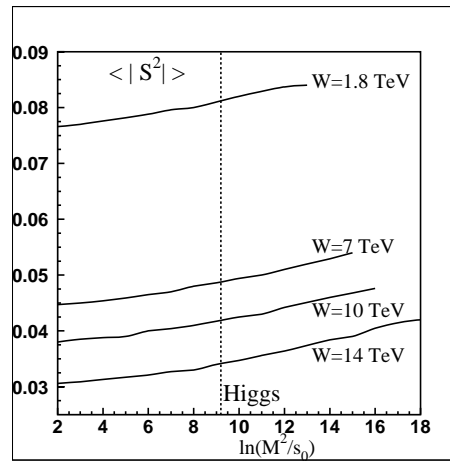
CALCULATED CROSS SECTIONS

The table displays GLM, KMR and Ostapchenko output results.

The figure shows GLM mass dependence of S_H^2. H=Higgs.

LHC DATA AND ITS INTERPRETATION

1)From The Tevatron To LHC:

Available predictions, regardless of the method with which they were obtained, are based on relatively low energy data analysis.

- The Tevatron data, on its own, does not have the resolution to discriminate between the soft Pomeron models I have discussed.
  Consequently, a successful reproduction of Tevatron data does not secure a similar success at the LHC.

- The early LHC cross section data published over the last few weeks can provide the extra resolution needed to discriminate between models and ideas. However, as long as the LHC volume of relevant data will be considerably smaller than the ISR-Tevatron data base, we shall need to apply more sophisticated methods in our data analysis.

2) Inclusive Pseudorapidity Distributions:

ALICE and CMS have just published the NSD charged multiplicity density $dN_{ch}/d\eta = (1/\sigma_{NSD})d\sigma/d\eta$, at central pseudorapidity $-2.5 \le \eta \le 2.5$.

This data provides an additional angle to assess the $I\!P$ models.

Regretfully, neither KMR nor Ostapchenko have any publications on this topic.

The following is a short summary of the GLM approach. **In the framework of Gribov's $I\!P$ calculus, single inclusive cross sections can be calculated using Mueller diagrams.** In the calculation, we have used the GLM $I\!P$ model fitted parameters, to which we have to add 3 additional phenomenological parameters:

$a_{I\!P I\!P}$ and $a_{I\!P R} = a_{R I\!P}$. They account for hadron emission from the $I\!P$ or Reggeon. Q is the average transverse momentum of the produced minijets with a mass $Q_0 Q$. In BNL minijet studies $Q_0 = 2$ GeV.
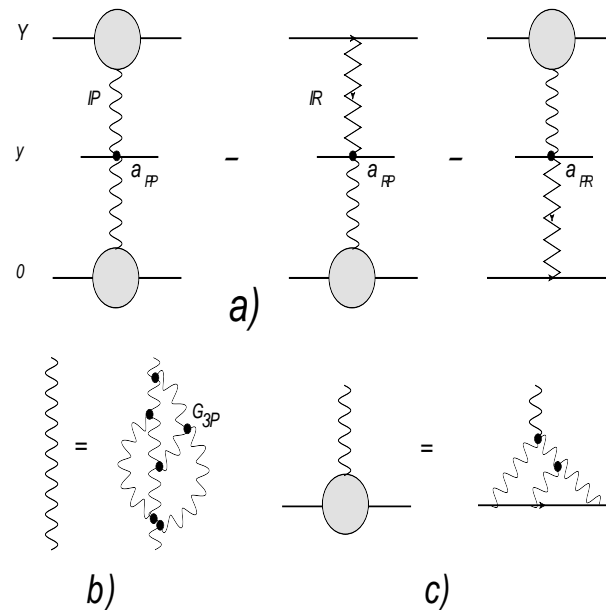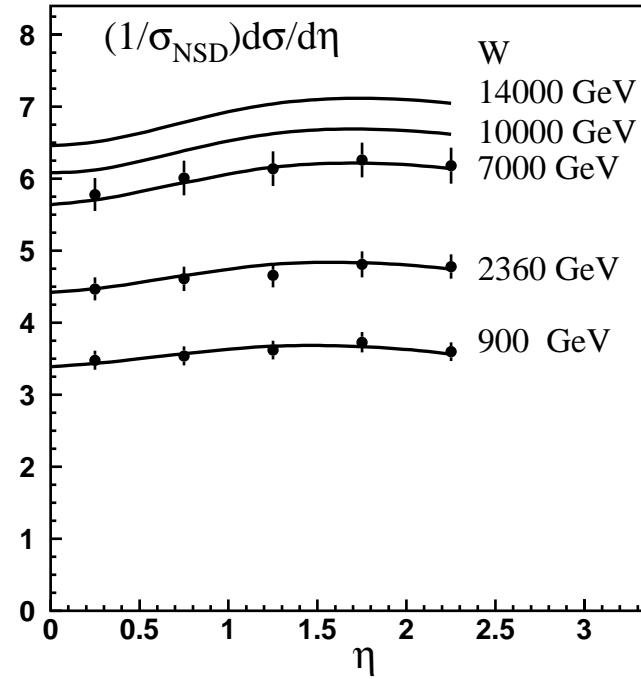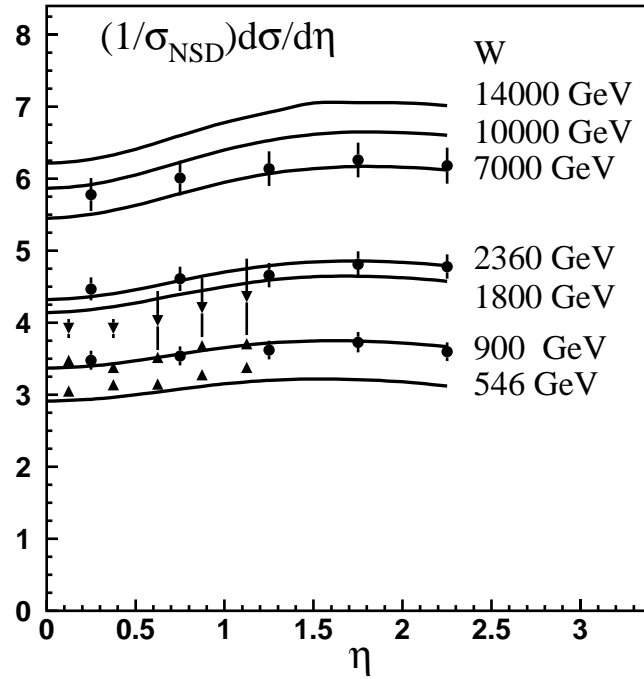
FIG. 1: a) Mueller inclusive diagrams, b) $I\!\!P$ Green function, c) $I\!\!P$-hadron vertex. A bold waving line $= I\!\!P$. A zigzag line $= R$.

The data base for this fit is obtained from a few experiments spread over many years with different approaches to their error estimates. We have fitted the data twice. Once, fitting the 546, 900, 1800, 2369, 7000 GeV data. The second fitting was confined to the very recent CMS data at 900, 2360, 7000 GeV. The 2 sets of fitted parameters are close but not identical. The difference between the 2 values of Q/Q_0 is significant for the CMS fits at small η.

Data	$a_{I\!\!P I\!\!P}$	$a_{I\!\!P R}$	Q_0/Q
CMS	0.390	0.186	0.427
All	0.413	0.194	0.356

$(1/\sigma_{NSD})d\sigma/d\eta$

W
14000 GeV
10000 GeV
7000 GeV

2360 GeV
1800 GeV

900 GeV
546 GeV

η

$(1/\sigma_{NSD})d\sigma/d\eta$

W
14000 GeV
10000 GeV
7000 GeV

2360 GeV

900 GeV

η

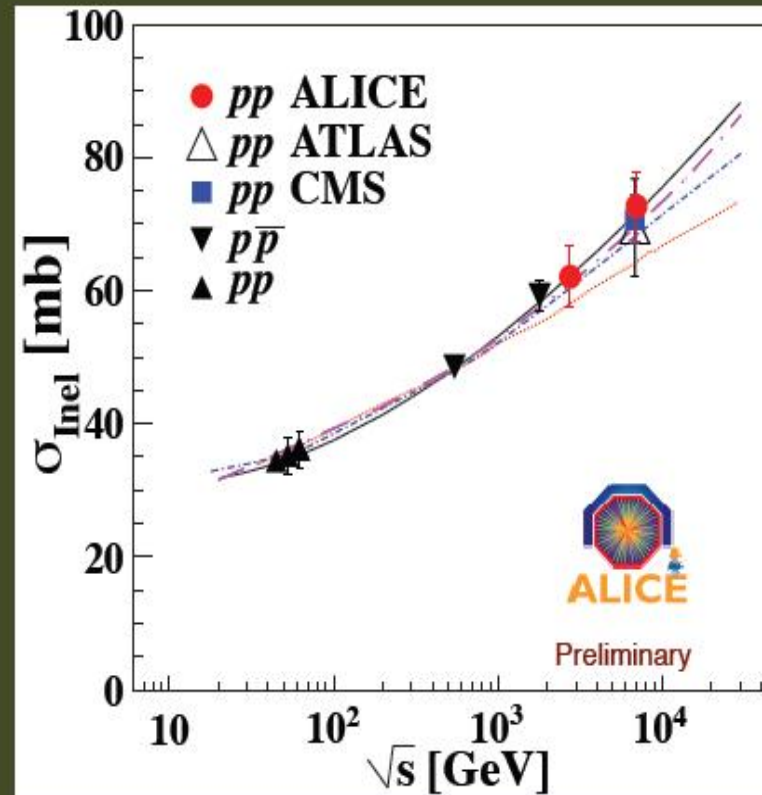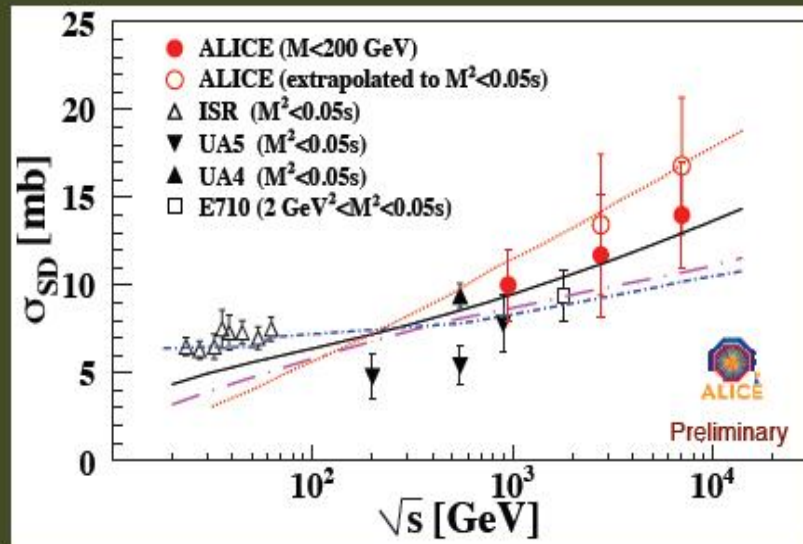| ATLAS10	ALICE11	Achilli et al.	Block-Halzen	GLM	Kaidalov el al.	KMR
$69.4 \pm 2.4 \pm 6.9$	$72.7 \pm 1.1 \pm 5.1$	60-75	69	68.3	70	62.6-67.1

3) Inelastic Cross Sections:

- The measurement of σ_{inel}, the inelastic cross section, is relatively easy. Indeed, it was measured by **ALICE, ATLAS and CMS.**

- **Theoretically, $\sigma_{inel} = \sigma_{tot} - \sigma_{el}$ can be predicted not only by the complicated multi channel unitary models but, also, by single channel models in which the GW mixing is ignored.** Recall, though, that single channel models are prone to over estimate the survival probability.

- The table compares between the **ATLAS10** and **ALICE11** measurement at **7 TeV** and **5 model predictions.**

CONCLUSIONS

- The main issue I have discussed is the conceptual changes in the Pomeron model once s and t unitarity are considered. Its main feature is a large $\triangle_{I\!P}$ and a diminishing $\alpha'_{I\!P}$. The new architecture of the $I\!P$ model radically changes the traditional roll of the $I\!P$ Regge trajectory.

- The new parameterization of the soft $I\!P$ trajectory is close to the parametrization of the BFKL Pomeron. It is, thus, tempting to consider a single Pomeron (GLM) or a combination of several BFKL Pomerons (KMR).

- A consequence of the above is that the t channel interactions become significant above the Tevatron. As a result, the validity of simple minded extrapolations from the ISR-Tevatron to LHC is questionable.

Comparison with other experiments and models